Protective role of *Achyranthes bidentata* polysaccharides against chondrocyte extracellular matrix degeneration through lncRNA GAS5 in osteoarthritis

CHANGLONG FU[1,2*], ZHIWEI QIU[1,2*], YANFENG HUANG[1,2*], YANGYANG MEI[3], QING LIN[1,2], JIANWEI ZENG[1,2], WEIHONG ZHONG[4,5] and DEZUN MA[1,2]

[1]Academy of Integrative Medicine, Fujian University of Traditional Chinese Medicine; [2]Fujian Provincial Key Laboratory of Integrative Medicine on Geriatrics; [3]Faculty of Nursing, Fujian Health College, Fuzhou, Fujian 350122; [4]Orthopedics Department, Rehabilitation Hospital Affiliated to Fujian University of Traditional Chinese Medicine; [5]Fujian Key Laboratory of Rehabilitation Technology, Fuzhou, Fujian 350003, P.R. China

Received January 14, 2022; Accepted May 31, 2022

DOI: 10.3892/etm.2022.11459

Abstract. *Achyranthes bidentata* polysaccharides (ABPS) is an active ingredient of the flowering plant *Achyranthes bidentata* that has been previously reported to be effective for the treatment of osteoarthritis (OA). However, the underlying molecular mechanism remain to be fully clarified. Emerging studies have shown that the long non-coding RNA (lncRNA) growth arrest-specific transcript 5 (GAS5) is involved in the pathogenesis of OA. Therefore, the present study aimed to investigate the potential mechanism of ABPS by focusing on its effects on the regulation of chondrocyte extracellular matrix (ECM) homeostasis, with particular emphasis on lncRNA GAS5. In the present study, the modified Hulth method was used to construct OA rats, which were gavaged with 400 mg/kg ABPS for 8 weeks. Histopathological changes in cartilage and subchondral bone were evaluated by hematoxylin-eosin staining and Safranin O-fast green staining. In *in vitro* experiments, IL-1β-treated chondrocytes were infected with Lenti-lncRNA GAS5. Fluorescence in situ hybridization assay was performed to measure the expression of the lncRNA GAS5 in chondrocytes. Moreover, the relative expression level of lncRNA GAS5 in cartilage tissue and chondrocytes was detected using reverse transcription-quantitative PCR. Western blot analysis was used to detect protein expression levels of MMP-9, MMP-13, TIMP-1, TIMP-3 and type II collagen in cartilage tissue and chondrocytes. The results indicated that ABPS delayed the degradation of the ECM by chondrocytes in addition to reducing lncRNA GAS5 expression both *in vivo* and *in vitro*. Furthermore, silencing of lncRNA GAS5 expression in IL-1β-treated chondrocytes downregulated the protein expression of MMP-9 and MMP-13 whilst upregulating the expression of tissue inhibitor matrix metalloproteinase (TIMP)-1, TIMP-3 and type II collagen. To conclude, the present study provides evidence that ABPS can inhibit the expression of lncRNA GAS5 in chondrocytes to regulate the homeostasis of ECM, which in turn may delay the occurrence of cartilage degeneration during OA.

Correspondence to: Dr Dezun Ma, Academy of Integrative Medicine, Fujian University of Traditional Chinese Medicine, 1 Qiuyang Road, Fuzhou, Fujian 350122, P.R. China
E-mail: 2021025@fjtcm.edu.cn

*Contributed equally

Abbreviations: ABPS, *Achyranthes bidentata* polysaccharides; OA, osteoarthritis; lncRNA, long noncoding RNA; FISH, fluorescence *in situ* hybridization; HE, hematoxylin-eosin; ECM, extracellular matrix; TIMPs, tissue inhibitor of metalloproteinases

Key words: Achyranthes bidentata polysaccharides, osteoarthritis, extracellular matrix, long non-coding RNA growth arrest-specific 5

Introduction

Osteoarthritis (OA) is a joint disease that is caused by a variety of pathogenic factors. One of the main pathological features of OA is the gradual degradation of hyaline cartilage (1,2). Other manifestations include increased risk of fracture or the loss of articular cartilage, exposure of the subchondral bone and the formation of osteophytes (3). The articular cartilage, which is the hyaline cartilage, mainly consists of type II collagen and proteoglycans (4). During the onset of OA, type II collagen is degraded and proteoglycans are lost in large quantities, resulting in reductions in compressive strength and elasticity of the cartilage whilst increasing the pressure load, which aggravates mechanical damage (5). Patients with OA predominantly experience arthralgia, swelling, deformity, limited range of motion and loss of function, which seriously affects their quality of life, particularly among the middle-aged and elderly population (6,7).

Achyranthes bidentata has been extensively used for the treatment of OA due to its reported anti-inflammatory and antioxidant properties (8,9). *Achyranthes bidentata* polysaccharides (ABPS) is a water-soluble form of fructan that can be extracted from the *Achyranthes bidentate* plant (10). The

chemical structure of ABPS is dominated by furan rings, where its molecular weight is in the range of 1.4-3.4 kDa (11). ABPS has been widely applied for the treatment of bone-related diseases, such as osteoporosis and OA, due to its observed protective effects on the bone (12,13). As an anti-inflammatory agent, ABPS has been previously shown to interfere with the inflammatory activation that occurs during OA and the metabolic pathway of arachidonic acid (13). In a castrated rat model of osteoporosis, ABPS has been documented to significantly increase the bone-mineral content and biomechanical properties of the femur, which protected these rats from osteoporosis by stimulating bone formation (14). ABPS has also been shown to effectively promote the proliferation of chondrocytes by promoting G_1/S cell cycle progression, suggesting that ABPS may be a potential drug for the treatment of OA (15). However, the precise role and mechanism of action mediated by ABPS on OA remains unclear. Therefore, the present study investigated the specific mechanism of action ABPS on OA from the perspective of cartilage matrix homeostasis.

Emerging studies have shown that long non-coding RNAs (lncRNA) serve an important role in OA (16). In particular, the expression of the lncRNA growth arrest-specific transcript 5 (GAS5) has been found to be upregulated in the OA cartilage, which may exacerbate cartilage degeneration by promoting chondrocyte apoptosis (17). Therefore, the aim of the present study is to verify if the mechanism of ABPS on OA acts through lncRNA GAS5 and associated signaling molecules. This hypothesis was further tested using viral transfection for *in vivo* and *in vitro* experiments.

Materials and methods

Main reagents. ABPS (cat. no. B25872; Lot no. C22M7Y11580; Shanghai Yuanye Bio-Technology Co., Ltd). HE Staining Kit (cat. no. G1120; Lot no. 20180111; Beijing Solarbio Science & Technology Co., Ltd.). RIPA buffer (Beyotime Institute of Technology). PMSF (Beijing Solarbio Science & Technology Co., Ltd.). HiScript II 1st Strand cDNA Synthesis Kit (cat. no. R211-02; lot no. L/N:7E460H0; Vazyme Biotech Co., Ltd.). ChamQ Universal SYBR® qPCR Master Mix (cat. no. Q711-02; lot no. 7E410L0; Vazyme Biotech Co., Ltd.). MMP-9 (1:1,000; cat. no. ab76003; lot. no. GR324586-17; Abcam) primary antibody. MMP-13 (1:1,000; cat. no. 18165-1-AP, lot no. 00089106; Proteintech Group, Inc.) primary antibody. Tissue inhibitor of metalloproteinases (TIMP) 1 (1:1,000; cat. no. 16644-1-AP, lot. no. 00023865; Proteintech Group; Inc.) primary antibody. TIMP-3 (1:1,000; cat. no. 10858-1-AP, lot. no. 00091772; Proteintech Group, Inc.) primary antibody. Type II collagen (1:1,000; cat. no. ab188570, lot. no. GR3233600-8; Abcam) primary antibody. GAPDH rabbit polyclonal (1:1,000; cat. no. 10494-1-AP, cat. no. 00098110; Proteintech Group, Inc.) primary antibody. Goat Anti-Rabbit IgG (H+L) HRP conjugate (1:5,000; cat. no. SA00001-2; lot no. 20000258; Proteintech Group, Inc.) secondary antibody.

In vivo experiments. Animals were purchased from Shanghai Slack Laboratory Animal Co., Ltd. [Qualification No. SCXK (Shanghai) 2017-0005]. The temperature of the rearing environment was controlled at 23-25˚C, the humidity was 55-60%, the air was changed 16 times per h and the cyclic light conditions were automatically controlled at 12-h light/dark cycle. Experimental animals were provided food and water *ad libitum*. The breeding environment and dietary conditions of experimental animals are in line with the standards of the Experimental Animal Center of Fujian University of Traditional Chinese Medicine [license no. SYXK (Fujian; 2019-0007)]. In total, 45 2-month-old male Sprague-Dawley rats were fed adaptively during the first week, weighed, numbered and randomly divided into three groups. Randomization was performed using the 'RAND' function on Microsoft Excel (Microsoft Corporation) 2016 (18). Ultimately, 45 animals were assigned to each of the three following groups: Normal group (n=15), model group (n=15) and the ABPS group (n=15). An OA model was constructed according to a modified version of the Hulth method (19). The model group and the ABPS group were modeled by the modified Hulth method. In the normal group, only the skin was incised (the joint capsule and ligament were not incised) and finally sutured. The rats were first anaesthetized with 5% isoflurane at 2 l/min O_2 using a mask and maintained at 2%. They were then fixed in a supine position, depilated at the right knee and locally disinfected with 75% ethanol. A 1-cm longitudinal incision was then made on the medial side of the right knee. The medial collateral ligament and the anterior cruciate ligament were cut through the incision, and the medial meniscus was removed. Finally, the joint capsule and the skin were sutured and disinfected again with 75% ethanol. After modeling, penicillin $20x10^4$ U was injected intraperitoneally for 3 days to prevent site infection. From week 6 after modeling, the normal and model groups were given normal saline at a dose of 10 ml/(kg·day), whereas the ABPS group was given a clinically equivalent dose of ABPS at 400 mg/(kg·day) (20). Almost all previous studies opted for the oral intake method for ABPS for treating bone diseases, such as osteoporosis (12,20,21) and OA (13). Since the present study was focused on exploring the protective mechanism of ABPS against OA, the most common delivery method, which is the oral gavage, was adopted for the rats. The intragastric dose was adjusted on a weekly basis according to body weight to 10 ml/(kg·day). The gavage time was between 9 AM and 1 PM. The daily gavage sequence was random, where each animal was treated at a different time on each day. Rats were dosed six times a week for a total of 8 weeks of treatment.

The experiment lasted for a total of 14 weeks. After ABPS or vehicle treatment, each group was deeply anesthetized by 5% isoflurane followed by euthanasia using cervical dislocation. All the experiments were performed under the ethical principles of animal experiments to reduce the suffering of experimental animals. All experimental procedures were approved by the Animal Use and Care Committee of Fujian University of Chinese Traditional Medicine (approval no. 2017026).

Histological evaluation. Knee joint cartilage tissue and subchondral bone tissue were first fixed in 4% paraformaldehyde at room temperature for 2 days and placed in ethylenediaminetetraacetic acid disodium salt (EDTA-2Na) for 8 weeks at room temperature. Tissues were sequentially placed in 50, 70, 80, 95, 100% ethanol to complete dehydration for 45 min at room temperature for each gradient. The embedding frame containing the tissue was then placed in

xylene I and xylene II in sequence, and placed in a 65˚C oven for 1 h each. Finally, the dissolved paraffin is introduced into the embedding frame, and after the wax block is completely solidified, the embedding frame was disassembled and the wax block taken out. Paraffin blocks were cut into 8-μm serial sections for standard HE staining and Safranin O-fast green staining (Beijing Solarbio Science & Technology Co., Ltd.). In HE staining, after the paraffin sections were baked in a 65˚C oven for 30 min, they were placed at room temperature with xylene I and xylene II for 5 min each. Then rehydrate with graded ethanol of 100, 95, 85 and 75% for 3 min. Then, a series of operations such as hematoxylin staining (5 min), differentiation solution (2 min) and eosin staining (1 min) were used, and finally dehydration and mounting were performed. In Safranin O-fast green staining, the paraffin sections were first baked in a 65˚C oven for 30 min and then the paraffin sections were deparaffinized and rehydrated. Subsequent steps were carried out at room temperature. Weigert staining was performed for 3 min, acid differentiation solution for 10 sec, and fast green staining solution for 5 min. Following washing with weak acid solution for 10 sec, staining in safranine staining solution for 5 min and finally dehydrating and sealing. Histopathological changes in the cartilage and subchondral bone were observed under a light microscope (DM4000 B; Leica Microsystems GmbH). Original magnification, x200. Rat tissue sections were evaluated using the modified Wakitani scoring system (22,23), which consists of the following five items: Cell morphology (0-4), matrix-staining or metachromatic staining (0-3), surface regularity (0-3), thickness of the cartilage (0-2) and integration of repaired tissue to the surrounding articular cartilage (0-2). The total score is 0 to 14 points (n=3 rats in each group), divided into three groups of three repetitions, each repetition of three fields of view, for a total of nine fields of view.

LncRNA GAS5 in OA cartilage as detected using reverse transcription-quantitative PCR (RT-qPCR). Total RNA was extracted using an RNA isolator Total RNA Extraction Reagent (cat. no. R401-01; Lot no. 7E490L0; Vazyme Biotech Co., Ltd.). The total RNA was then reverse transcribed into cDNA according to the protocols of the reverse transcription kit. Next, the cDNA was configured and loaded according to the steps of the qPCR reaction kit. Gene expression was detected on the Bio-Rad CFX96 real-time fluorescent quantitative PCR instrument. The following primers pairs were used for the qPCR: LncRNAGAS5 (Rat) forward, 5'-GGGATG GTGGAGTTTGAATCAG-3' and reverse, 5'-GCTTGCCAT GCCTTCAGTTA-3' and GAPDH forward, 5'-ACGGCAAGT TCAACGGCACAG-3' and reverse, 5'-GAAGACGCCAGT AGACTCCACGAC-3'.

Western blotting for the in vivo experiment. The rats were deeply anesthetized by the inhalation of 5% isoflurane, before the cartilage tissue from the right femoral condyle and tibial plateau was obtained. Total protein was then extracted from the cartilage tissue using the RIPA buffer (Beyotime Technology, Shanghai, China). The protein concentration was determined using the BCA method, before 20 μg protein sample was loaded into each well of a 10% sodium lauryl sulfate-polyacrylamide gel, after which electrophoresis separation was performed. The semi-dry proteins were then transferred onto a PVDF membrane, followed by washing with TBST containing 0.05% Tween 20. The membrane was then incubated in NcmBlot Blocking Buffer (Alexan Biotech Co., Ltd.) at room temperature for 2 h. Next, the membrane was incubated in either of the following primary antibodies overnight at 4˚C: (Rabbit polyclonal) MMP-9, MMP-13, TIMP-1, TIMP-3, type II collagen and GAPDH. The following day, the membranes were washed three times with TBST to remove any residual antibodies. The membranes were then incubated in the Goat Anti-Rabbit IgG (H+L), HRP conjugate for 1 h at room temperature, followed by another round of washing with TBST. An appropriate amount of BeyoECL Plus (Beyotime Institute of Biotechnology) was then added to the membrane and the reaction was stopped after 1 min. The membrane was then exposed and developed. Using Image Lab software version 3.0 (Bio-Rad Laboratories, Inc.), GAPDH was used as the internal reference to analyze the gray value ratio of the target protein.

Chondrocyte culture. The rats were anesthetized under 5.0% isoflurane and sacrificed by cervical dislocation after they lost consciousness. The articular cartilage was then separated from both knee joints, transferred to PBS containing penicillin and streptomycin and washed three times. The cartilage was cut into ~1 mm^3, then 5 ml of 0.2% type II collagenase was added and put into a 37˚C, 5% CO_2 incubator for digestion for 4 h and then transferred to a sterile centrifuge tube for centrifugation (137.4 x g for 3 min in a 4˚C centrifuge.). The supernatant was removed, 5 ml of DMEM containing 10% FBS was added to the lower sedimentary tissue to terminate the digestion, and it was transferred to a culture flask for culture at 37˚C in an incubator containing 5% CO_2. The culture medium was changed every 2 days and primary chondrocytes were finally obtained. Type II collagenase, FBS and DMEM were obtained from HyClone (Cytiva). In culture, the large number of dedifferentiated chondrocytes were subsequently passaged three to four times, after which the chondrocyte phenotype was lost. Therefore, only second-generation chondrocyte cultures were used for the present study.

Construction of lncRNA GAS5-knockdown chondrocytes. A third-generation lentiviral packaging system was used in the present study to infect chondrocytes with Lenti-lncRNA GAS5. The lentivirus was packaged by Zolgene Biotechnology Co., Ltd. lncRNA GAS5-shRNA (cat. no. ZL-21P1048). 293FT cells (Invitrogen, USA) were plated into 10 cm-dish (5 million/dish) and incubated at 37˚C and 5% CO_2 in DMEM (Invitrogen; Thermo Fisher Scientific, Inc.). On the next day, the 293FT cells were ~80% confluent and the lentiviral transfection was performed by adding pMDLg/pRRE (6 μg), pRSV-Rev (3 μg), pMD2.g (2 μg), shuttle plasmid (9 μg) and Lipofectamine® 3000 (Invitrogen; Thermo Fisher Scientific, Inc.; 40 μl). The full name of the shRNA plasmid was plvx-shRNA-puro. Following 72 h incubation at 37˚C, the 293FT lentiviral supernatant was harvested and used at 1, 4, 8, 12 and 16 multiplicities of infections (MOI) to transfect the chondrocyte cells in the log phase of the growth plated in six-well plates, using 5 μg/ml of polybrene per well at 37˚C overnight. After 6 h of infection, 1 ml DMEM (Invitrogen; Thermo Fisher Scientific, Inc.) containing

10% FBS was added into each well and incubated at 37˚C overnight. After 24 h of transfection, the virus-containing medium was aspirated before 2 ml fresh medium was added and the culturing was continued. GFP was transiently expressed 50 h after transfection, and the green fluorescent signal observed under a fluorescence microscope (Carl Zeiss AG; magnification, x100). At least three fields of view were checked for each MOI value and the MOI value with the fluorescence area >80% and the best cell viability was generally chosen.

Fluorescence in situ hybridization (FISH). FISH assay was performed to measure the local expression of the lncRNA GAS5 in chondrocytes. In the present study, GAS5 RNA probe labeled by digoxigenin (DIG) were selected. All probes were custom synthesized by General Biosystems (Anhui) Corporation Limited. Gas5-rat probe: 5'-CCACCATCCCATTTTCTGGCT TCCCATTCT(TTTCATCATCATACATCATCAT)30-3'; and DIG-labeled probe: 5'-DIG-TTATGATGATGTATGATGAT GT-3'. (TTTCATCATCATACATCATCAT) 30-3' is a repeated nucleic acid sequence with 30 repeats. Gene ID for GAS5: 81714. The second-labeled probe had a digoxigenin label, and the second-labeled probe was complementary to the repeating sequence of the first-labeled probe and can be completely combined. The GAS5 probe sequence was untagged. The slides were immersed in chondrocyte culture medium to transfer chondrocytes to the slides for growth. Slides were fixed with 4% paraformaldehyde (DEPC) for 20 min at 37˚C and washed with PBS (pH 7.4) in a decolorizing shaker. Proteinase K (20 μg/ml; cat. no. G1205; Wuhan Service bio Technology Co., Ltd.) was added to cover the tissue and incubated at 37˚C for 2 h. The hybridization buffer without probe (cat. no. G3016-3; Wuhan Service bio Technology Co., Ltd.) was added onto the specimen and incubated at 37˚C for 1 h. The solution covering the samples was then replaced with hybridization buffer containing GAS5-rat probe at a concentration of 500 nM and hybridized overnight in a humidified chamber at 42˚C. After removing the hybridization solution, gradient washes were performed under saline-sodium citrate (SSC) buffer (2X SSC at 37˚C for 10 min, 1X SSC at 37˚C for 10 min, and 0.5X SSC at 37˚C for 10 min). The DIG-labeled (1:400) probe was added dropwise and incubated at 42˚C for 3 h. The blocking solution (Wuhan Service bio Technology Co., Ltd.) was added to the specimen and incubated at room temperature for 30 min. The blocking solution was replaced by the anti-DIG-HRP antibody (1:10,000; cat. no. 200-032-156; Jackson ImmunoResearch Laboratories INC.) and incubated at 37˚C for 40 min, before the specimen was washed four times for 5 min in PBS. The sample was dried and CY3-TSA reagent added to the sample and the reaction was performed at room temperature for 5 min in the dark. After washing with PBS, the nuclei were counterstained with DAPI and incubated in the dark for 8 min. After rinsing, anti-fluorescence quenching mounting medium was added dropwise to mount the slides. (CY3-TSA reagent, DAPI staining solution and anti-fluorescence quenching mounting medium were purchased from Wuhan Service bio Technology Co., Ltd). Imaging was performed using a fluorescence microscope (magnification, x100).

Relative expression of lncRNA GAS5 in lncRNA GAS5-silenced chondrocytes. RT-qPCR was performed to measure the relative expression of the lncRNA GAS5 in the cultured chondrocytes transfected with or without the sh-lncRNA GAS5. For this experiment, cultured chondrocytes were divided into the following groups: blank + Lenti-control, blank + Lenti-lncRNA GAS5, IL-1β + Lenti-NC, and IL-1β + Lenti-lncRNA GAS5 group. Chondrocytes were treated with 10 ng/ml IL-1β (cat. no. MKCL5731; MilliporeSigma) at 37˚C for 24 h. The RT-qPCR protocol for *in vitro* cell experiments was the same as that used for the *in vivo* samples described above.

Protein expression of MMP-9, MMP-13, TIMP-1, TIMP-3 and type II collagen in lncRNA GAS5-silenced chondrocytes. *In vitro* cell experiments used the same western blotting protocol as described above for *in vivo* samples.

Relative expression of lncRNA GAS5 in IL-1β-treated chondrocytes following ABPS treatment. Cultured chondrocytes were divided into the following treatment groups: Control group, IL-1β group (24) and ABPS groups (15). The IL-1β group was treated with 10 ng/ml IL-1β at 37˚C for 24 h, and the ABPS group was treated with 50, 100 and 150 μg/ml ABPS at 37˚C for 48 h, respectively. The RT-qPCR protocol for *in vitro* cell experiments is the same as that used for the *in vivo* samples described above. Total RNA was extracted using TRIzol reagent (Invitrogen; Thermo Fisher Scientific, Inc.) according to the manufacturer's protocol. Total RNA was reverse transcribed into cDNA. The subsequent RNA detection was performed according to the real-time quantitative PCR kit. Briefly, 5 μl RNA sample was mixed with DEPC water solution at a ratio of 1:10, before the optical density (OD) value was measured on a DNA quantitative photometer. The OD260/OD280 of the RNA sample was qualified to be between 1.8 and 2.0. A value <1.8 mean a higher ratio of proteins than the extracted mRNA, which was deemed to be of insufficient quality. After the reaction, RT-qPCR amplification and dissolution curves were confirmed before the results were quantified.

Protein expression of MMP-9, MMP-13, TIMP-1, TIMP-3 and type II collagen in IL-1β-treated chondrocytes after ABPS treatment. *In vitro* cell experiments used the same western blotting protocol as described above for *in vivo* samples. Protein was extracted from cultured chondrocytes by RIPA buffer to generate a cell lysate, before the protein concentration was subsequently determined using the BCA protein concentration assay. Electrophoresis, film transfer, sealing, primary antibody incubation, secondary antibody incubation, substrate color development, image acquisition by gel imaging analysis system and quantitative analysis of the absorbance value of each strip were used to calculate the ratio of each sample to an internal reference protein absorbance value.

Statistical analysis. Data were analyzed using the SPSS 26 software (IBM Corp.) and were presented as the mean ± standard deviation. The measurement data were tested using one-way analysis of variance followed by Tukey's post hoc test. Wakitani scores were analyzed by Kruskal-Wallis test followed by Dunn's post hoc test. $P<0.05$ was considered to indicate a statistically significant difference. Each experiment was replicated three times in the *in vitro* experiments. In the

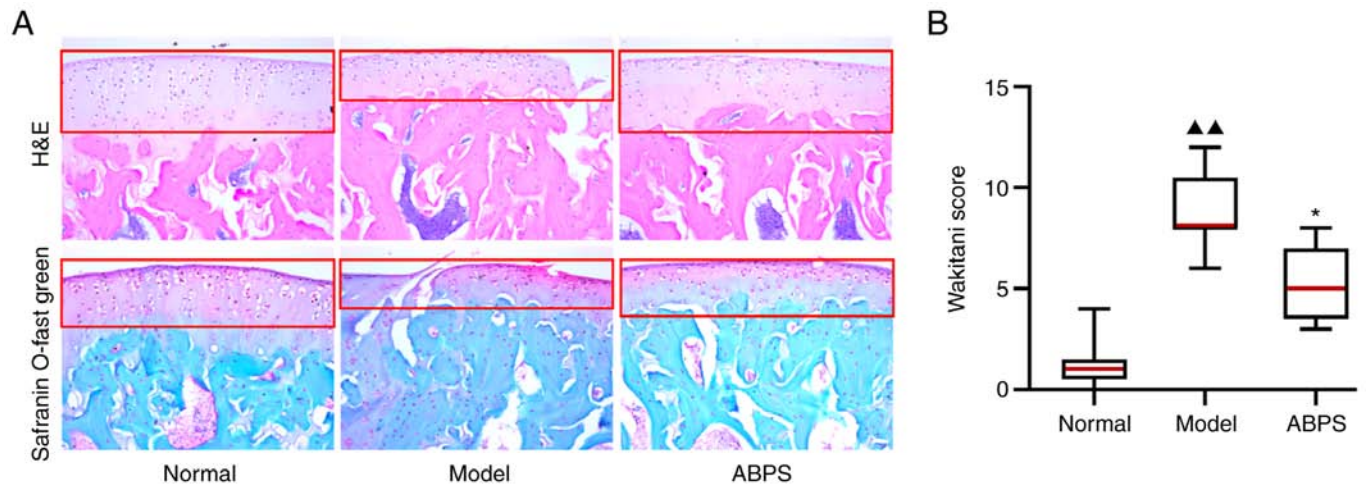

Figure 1. Histological evaluation of cartilage tissue. (A) HE staining and Safranin O-fast green staining of the cartilage tissue. Magnification, x200. (B) Histological scoring of cartilage repair according to the modified Wakitani score. Statistical analysis was performed using Kruskal-Wallis test followed by Dunn's post hoc test. ▲▲P<0.01 vs. Normal and *P<0.01 vs. Model.

in vivo experiments, 15 animals were assigned to each of the three following groups: Normal group, model group and the ABPS group.

Results

Histological evaluation results. The morphology of cartilage collected from control, OA model and ABPS-treatment groups was analyzed using HE-staining and Safranin O-fast green staining of tissue sections of the femoral condyle. The results demonstrated that the transparent cartilage layer in the OA model group displayed a rough surface and a discontinuous structure compared with that in the control and ABPS group, which received ABPS for eight weeks after OA modeling (Fig. 1A). Subsequently, the average modified Wakitani score in the model group was found to be significantly higher compared with that in the normal group (P<0.01), which was significantly reversed after ABPS administration (P<0.01; Fig. 1B). suggesting that ABPS can promote the repair of articular cartilage in rats with OA.

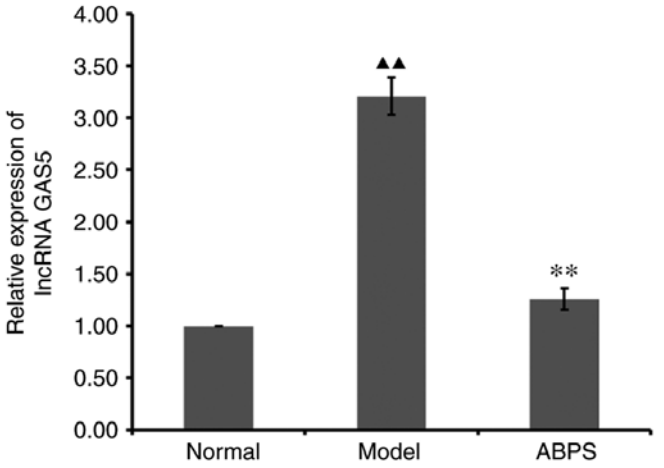

Figure 2. Reverse transcription-quantitative PCR of GAS5 expression for in vivo experiments. ▲▲P<0.01 vs. Normal and **P<0.01 vs. Model. lncRNA, long non-coding RNA; GAS5, growth arrest-specific transcript 5; ABPS, *achyranthes bidentata* polysaccharides.

RT-qPCR results of in vivo chondrocytes treated with ABPS. ABPS demonstrated regulatory ability in the expression of lncRNA GAS5 (Fig. 2). Compared with that in the normal group, the expression of lncRNA GAS5 in the OA cell model group was significantly increased (P<0.01; Fig. 2). Compared with that in the OA cell model group, the ABPS-treated group exhibited significantly reduced lncRNA GAS5 expression levels (P<0.01; Fig. 2).

Western blotting results after in vivo chondrocyte ABPS treatment. ABPS was demonstrated to exert a regulatory effect on the expression of MMP-9, MMP-13, TIMP-1, TIMP-3 and type II collagen in the cartilage of rats with OA (Fig. 3). Compared with that in the normal group, the expression of MMP-9 and MMP-13 in the model group was significantly increased, whereas that of TIMP-1, TIMP-3 and type II collagen was significantly downregulated (P<0.01; Fig. 3). Compared with that in the model group, the ABPS group showed significantly reduced MMP-9 and MMP-13 protein expression, whilst TIMP-1, TIMP-3 and type II collagen protein expression was significantly increased (P<0.05 or P<0.01; Fig. 3). These results suggest that ABPS can inhibit the expression of lncRNA GAS5 to delay the degradation of extracellular matrix (ECM) proteins by chondrocytes in OA.

Observation of primary chondrocytes. Chondrocytes were observed at different times of culture to monitor their proliferation and distribution characteristics in primary culture. The primary chondrocytes were isolated from normal rats and seeded into culture flasks, which displayed irregular, polygonal shapes after 6 days of culture (Fig. 4A). Primary chondrocytes began to grow in clusters on the 7th day, and the number of chondrocytes accounted for more than 90% of the space under the microscope (Fig. 4B). At first passage, the chondrocytes assembled into uniformly distributed cells by day 3 (Fig. 4C). After second passage, the chondrocytes occupied >80% of the

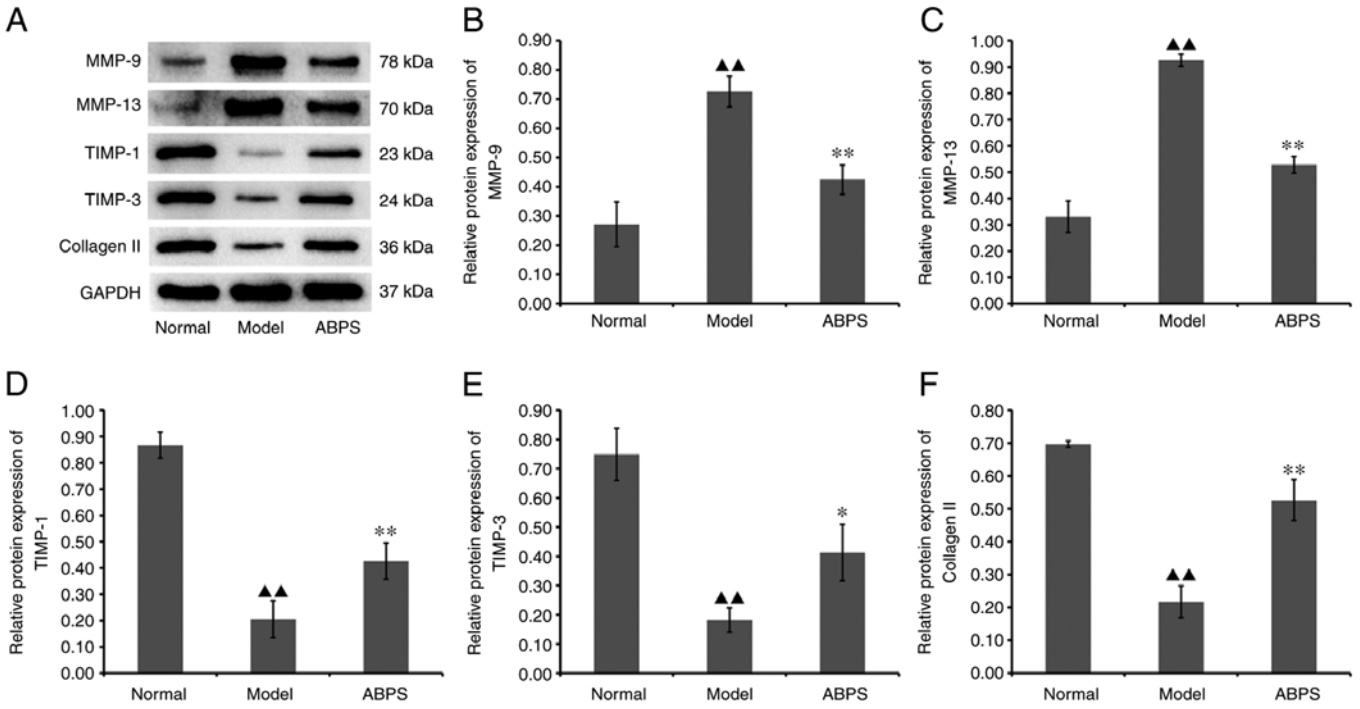

Figure 3. Western blotting of samples from *in vivo* experiments. (A) Western blot analysis of protein expression levels of MMP-9, MMP-13, TIMP-1, TIMP-3 and type II collagen. The protein expression levels of (B) MMP-9, (C) MMP-13, (D) TIMP-1, (E) TIMP-3 and (F) type II collagen were quantified. ▲▲P<0.01 vs. Normal; *P<0.05 and **P<0.01 vs. Model. TIMP, tissue inhibitor of metalloproteinase; ABPS, *achyranthes bidentata* polysaccharides.

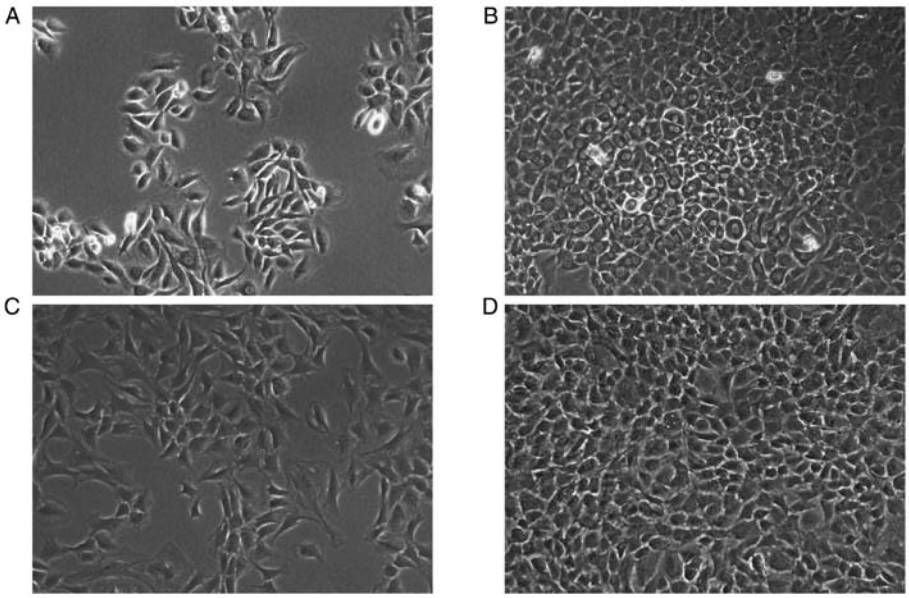

Figure 4. Morphological analysis of the chondrocytes. The chondrocytes cultured *in vitro* were observed using phase microscopy. Magnification, x100. (A) Images of the primary chondrocytes on day 6. (B) Images of primary chondrocytes on day 7. (C) First-passage chondrocytes after 3 days of culture. (D) Second-passage chondrocytes after 7 days of culture.

culture flask (Fig. 4D). Therefore, cultured second-generation primary chondrocytes were chosen to conduct subsequent experiments.

MOI of lncRNA GAS5 transfection. The logarithmic growth of chondrocytes whose density was 50% on the second culture day were seeded into six-well plates. Polybrene (5 μg/ml) and lncRNA GAS5 in 1, 4, 8, 12 and 16 MOIs were added into each of the six-well plates. Fluorescent images were taken 50 h after transfection. At MOI=8, the transfection efficiency of lncRNA GAS5 was considered to be high, at which point the survival rate of chondrocytes remained optimal (Fig. 5).

FISH results. LncRNA GAS5 was found to be mainly expressed in the chondrocyte cytoplasm, suggesting that lncRNA GAS5 could interact with other RNAs or proteins

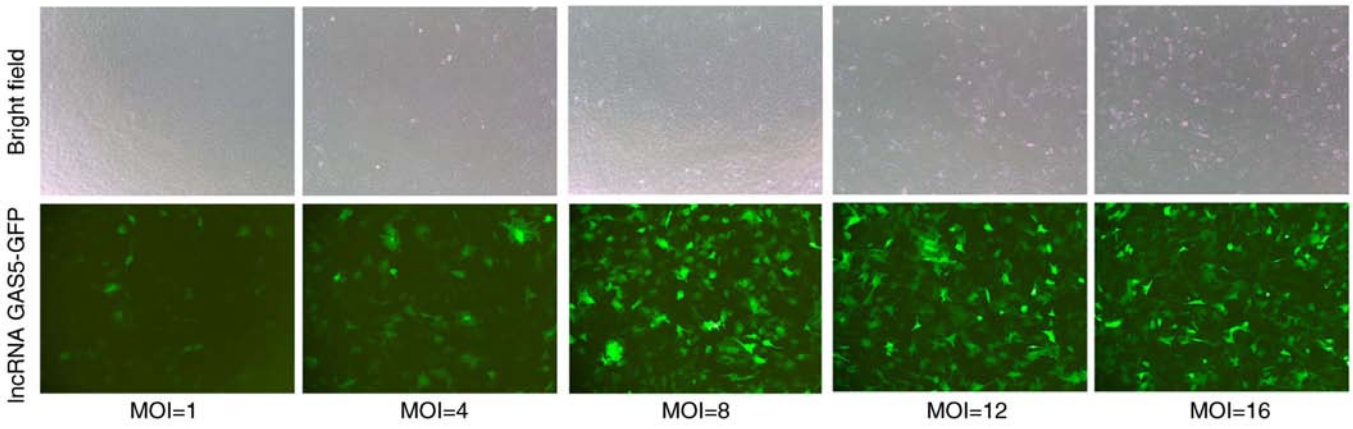

Figure 5. MOIs of chondrocytes transfected with shRNA lncRNA GAS5. LncRNA GAS5 transfection efficiency and chondrocyte survival rate at MOI of 1, 4, 8, 12 and 16. Magnification, x100. MOI, multiplicity of infection; shRNA, short hairpin RNA; lncRNA, long non-coding RNA; GAS5, growth arrest specific 5.

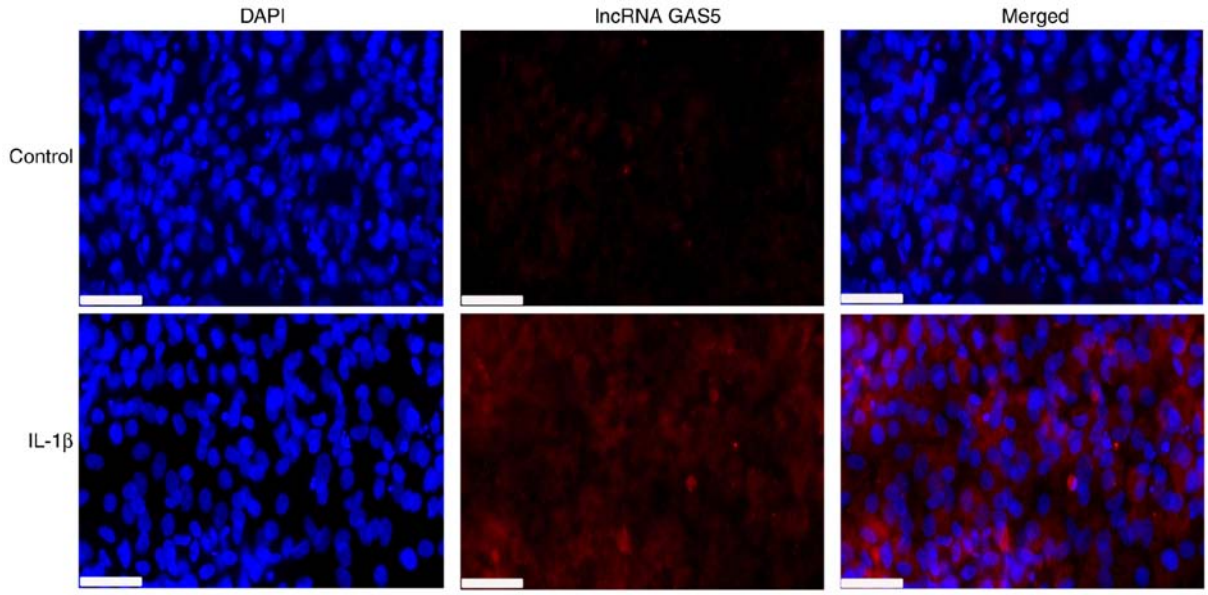

Figure 6. FISH analysis of lncRNA GAS5 expression. FISH analysis showed that lncRNA GAS5 is mainly expressed in the chondrocytes cytoplasm. Scale bar=40 μm. The relative expression levels of lncRNA GAS5 in the absence or presence of IL-1β treatment. FISH, fluorescence *in situ* hybridization; lncRNA, long non-coding RNA; GAS5, growth arrest specific 5.

in the cytoplasm of chondrocytes. IL-1β treatment was found to increase the expression of lncRNA GAS5 in chondrocytes (Fig. 6).

Sh-lncRNA GAS5 transfection can effectively regulate the homeostasis of ECM proteins by chondrocytes treated with IL-1β. The transfection efficiency of sh-lncRNA GAS5 was verified using RT-qPCR, which showed that the relative expression of lncRNA GAS5 in chondrocytes in the IL-1β + Lenti-lncRNA GAS5 group was significantly reduced compared with that in the IL-1β + Lenti-NC group (P<0.01). Compared with blank + Lenti-NC group, the relative expression of lncRNA GAS5 in chondrocytes of blank + Lenti-lncRNA GAS5 group was significantly decreased (P<0.01; Fig. 7).

After lncRNA GAS5 expression was knocked down, the expression of MMP-9, MMP-13, TIMP-1, TIMP-3 and type II collagen were normalized in chondrocytes treated with

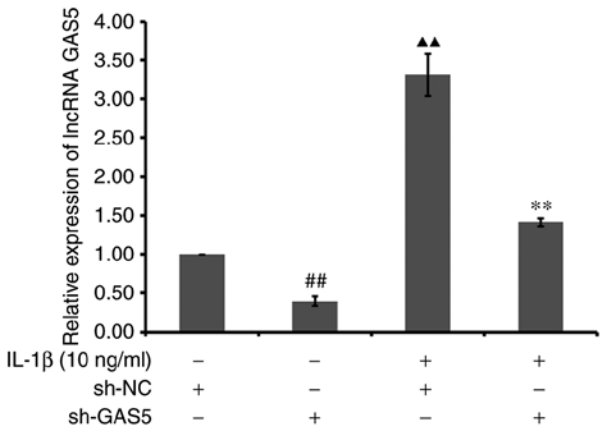

Figure 7. Effect of lncRNA GAS5 silencing on the relative expression of lncRNA GAS5 in chondrocytes induced by IL-1β. ##P<0.01 and ▲▲P<0.01 vs. blank + Lenti-NC; **P<0.01 vs. IL-1β + Lenti-NC. lncRNA, long non-coding RNA; GAS5, growth arrest specific 5; Lenti-NC, short hairpin negative control.

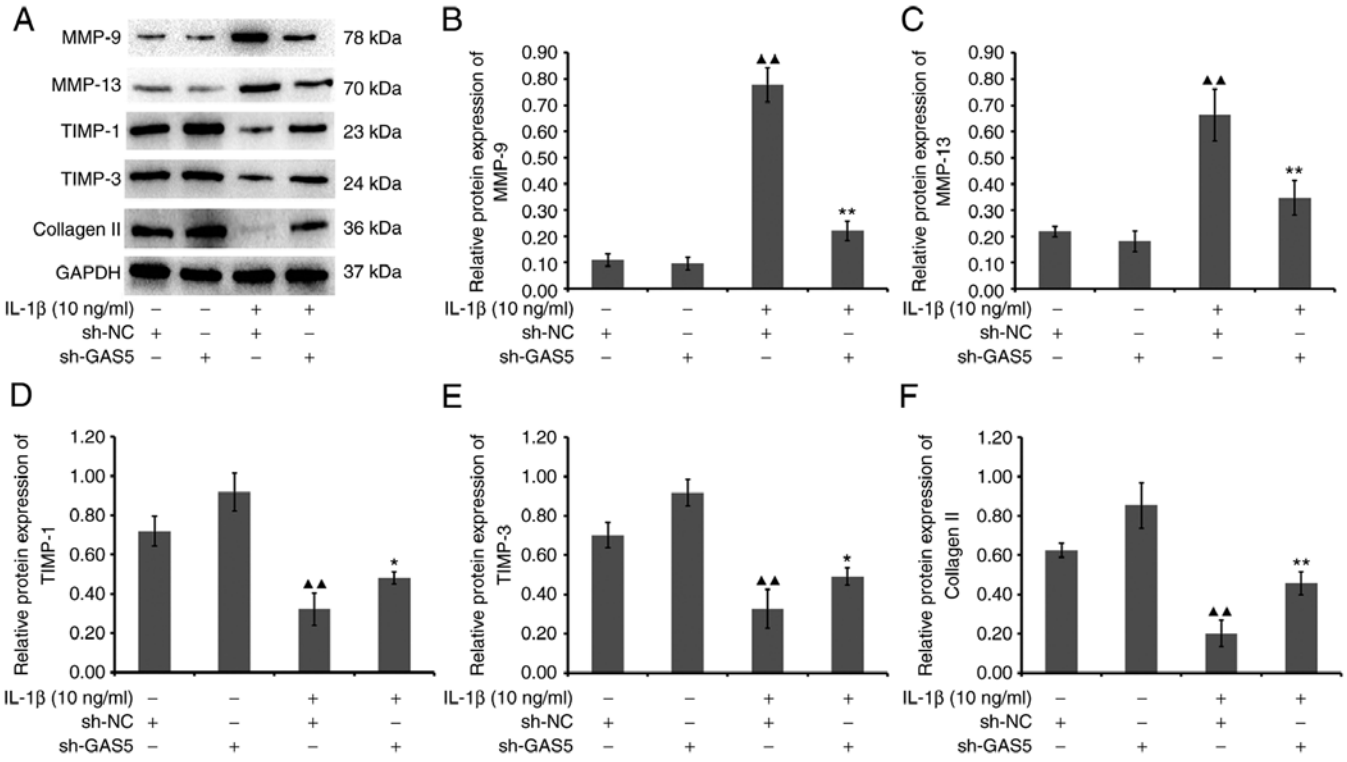

Figure 8. Effect of lncRNA GAS5 silencing on the protein expression levels of MMP-9, MMP-13, TIMP-1, TIMP-3 and type II collagen in chondrocytes. (A) Western blot analysis of the protein expression levels of MMP-9, MMP-13, TIMP-1, TIMP-3 and type II collagen. The protein expression levels of (B) MMP-9, (C) MMP-13, (D) TIMP-1, (E) TIMP-3 and (F) type II collagen were quantified. ▲▲P<0.01 vs. blank + Lenti-NC; **P<0.01 and *P<0.05 vs. IL-1β + Lenti-NC. lncRNA, long non-coding RNA; GAS5, growth arrest specific 5; TIMP, tissue inhibitor of metalloproteinase.

IL-1β. Compared with that in the blank+Lenti-NC group, the expression of MMP-9 and MMP-13 in the IL-1β + Lenti-NC group was significantly increased (P<0.01), whereas that of TIMP-1, TIMP-3 and type II collagen was significantly downregulated (P<0.01; Fig. 8). Furthermore, the expression of MMP-9 and MMP-13 in the IL-1β + Lenti-lncRNA GAS5 group was significantly decreased (P<0.01), whereas that of TIMP-1 (P<0.05), TIMP-3 (P<0.05) and type II collagen was upregulated (P<0.01), compared with that in the IL-1β + Lenti-NC group (Fig. 8). These results suggest that lncRNA GAS5 serves an important role in regulating chondrocyte physiology in terms of ECM homeostasis.

ABPS may regulate chondrocyte ECM homeostasis via lncRNA GAS5 in IL-1β-treated chondrocytes. RT-qPCR results showed that the relative expression of lncRNA GAS5 in the ABPS group was significantly reduced in the presence of IL-1β compared with that in the IL-1β alone group (P<0.01; Fig. 9). However, there was no statistical difference among the three groups of 50, 100 and 150 μg/ml ABPS, although it can be seen in Fig. 9 that 100 μg/ml of ABPS exerted the optimal response. Subsequent western blot analysis revealed that the expression of MMP-9 and MMP-13 in the ABPS group was significantly decreased (P<0.01), whereas that TIMP-1, TIMP-3 and type II collagen was significantly upregulated, compared with that in the IL-1β-alone group (P<0.01 or P<0.05; Fig. 10). These results suggest that ABPS can exert protective effects by regulating the expression of ECM-associated proteins in an *in vitro* model of OA chondrocytes.

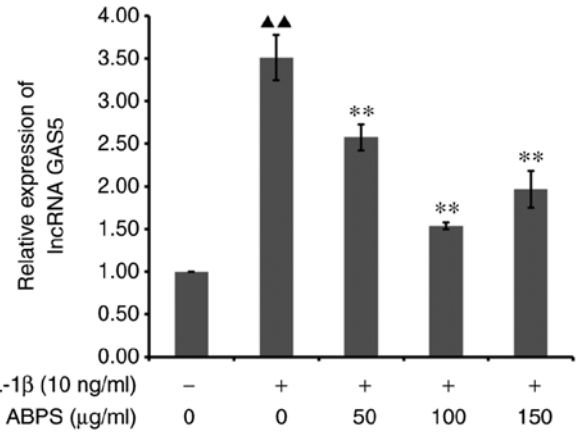

Figure 9. Effect of ABPS on the relative expression levels of lncRNA GAS5 in chondrocytes treated with IL-1β. ▲▲P<0.01 vs. Control. **P<0.01 vs. IL-β alone. ABPS, *achyranthes bidentata* polysaccharides; lncRNA, long non-coding RNA; GAS5, growth arrest specific 5.

Discussion

OA is a common chronic degenerative joint disease that seriously affects the quality of life of patients (25). *Achyranthes bidentata* is a commonly used traditional Chinese medicine that is widely used for the clinical treatment of OA. The China Food and Drug Administration has already approved numerous proprietary traditional Chinese medicines containing *achyranthes bidentata*, such as *Mailuoning* granules/injection/oral liquid and *Danxi* granules (9). An epidemiological

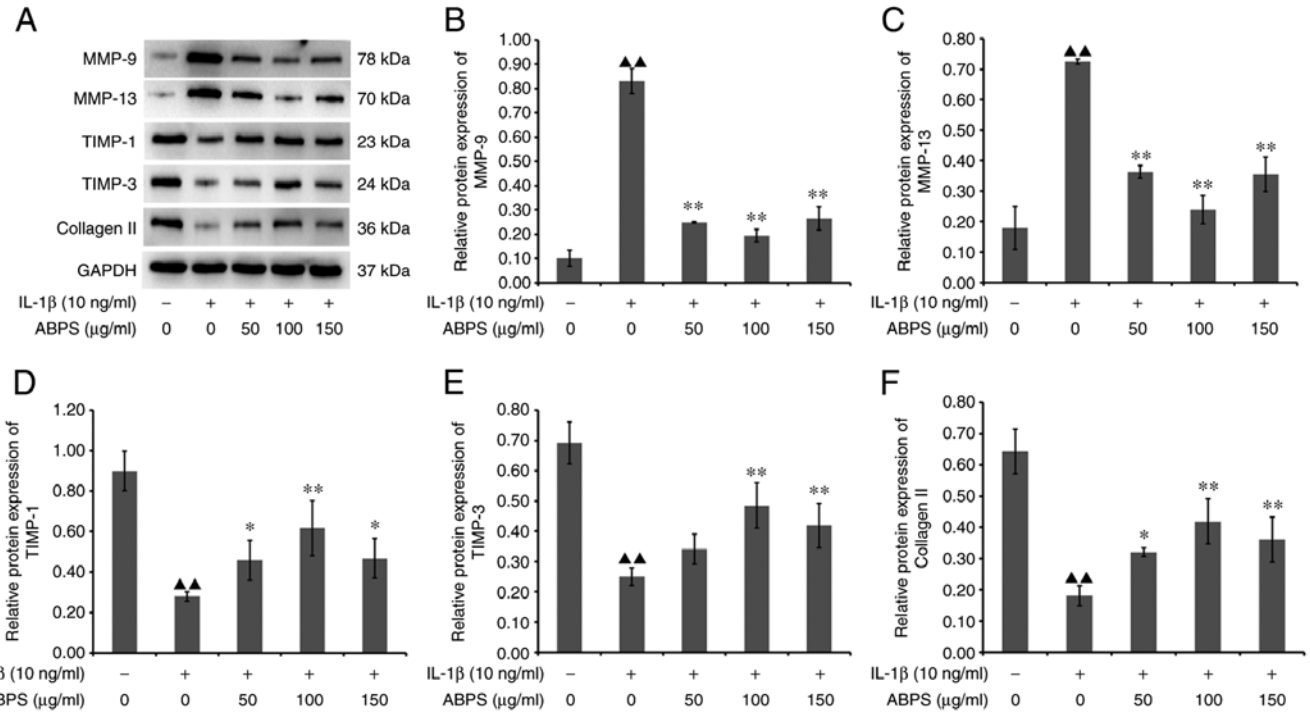

Figure 10. Effect of ABPS on the protein expression levels of MMP-9, MMP-13, TIMP-1, TIMP-3 and type II collagen chondrocytes treated with IL-1β. (A) Western blot analysis of the protein expression levels of MMP-9, MMP-13, TIMP-1, TIMP-3 and type II collagen. The protein expression levels of (B) MMP-9, (C) MMP-13, (D) TIMP-1, (E) TIMP-3 and (F) type II collagen were quantified. ▲▲P<0.01 vs. Control; **P<0.01 and *P<0.05 vs. IL-1β alone. ABPS, *achyranthes bidentata* polysaccharides; TIMP, tissue inhibitor of metalloproteinase.

survey on the use of traditional Chinese herbal medicine by patients with OA revealed that *achyranthes bidentata* is one of the most commonly prescribed Chinese herbs included in the Chinese herbal formula (23). As one of the bioactive components contained within *achyranthes bidentata*, ABPS has been reported to serve a key role in the regulation of bone metabolism (20). ABPS alleviates OA by reducing the inflammatory response through the arachidonic acid Pathway (11). In addition, it confers bone protective effects by promoting cell proliferation and bone formation (10). In the present study, it was found that ABPS can improve cartilage ECM homeostasis, thereby alleviating articular cartilage degeneration. This therefore provides a theoretical basis for the clinical application of *achyranthes bidentata* for OA treatment. A previous study has shown that ABPS can promote G_1/S cell cycle progression, which effectively promotes chondrocyte proliferation (15). In addition, ABPS can inhibit ECM degradation by increasing the expression of type II collagen (26). However, the mechanism of action remains unclear. The present study therefore investigated if ABPS can regulate chondrocyte physiology and ECM homeostasis through lncRNA GAS5 in an OA setting. The results of HE staining showed that the tangent line of the superficial layer in the ABPS group is parallel and continuous with the articular surface, where the transitional, radiation, calcified and other layers are relatively clear and identifiable, especially on the cartilage surface. Improvements in the cartilage matrix status was also observed; compared with the normal group, the thickness of the cartilage matrix was thinner in the model group and this trend was significantly improved after ABPS intervention. According to results from the morphological analysis, ABPS was found to delay cartilage degeneration by maintaining the homeostasis of ECM by chondrocytes. *In vivo* RT-qPCR and western blotting results showed that ABPS could inhibit the expression of lncRNA GAS5, while increasing the protein expression levels of TIMP-1, TIMP-3 and type II collagen and inhibiting the protein expression of MMP-9 and MMP-13 in cartilage tissue of OA rats.

Previous studies have shown that lncRNAs are involved in the pathological process of OA by regulating apoptosis and the homeostasis of cartilage ECM. The lncRNAs may accelerate the degeneration of articular cartilage by causing ECM degradation leading to abnormal cartilage remodeling (27,28). A previous study has found that the expression of the lncRNA GAS5 is upregulated in cartilage tissues with OA (29). RT-qPCR and FISH analysis revealed that the relative expression of lncRNA GAS5 was markedly increased in IL-1β-treated chondrocytes, which was mainly localized to the cytoplasm of chondrocytes. Tan *et al* (30) previously revealed that GAS5 is mainly located in the cytoplasm of nucleus pulposus cells in a model of intervertebral disc degeneration, such that GAS5 knockout can ameliorate nucleus pulposus cell degeneration by increasing ECM synthesis. Therefore, it could be speculated that ABPS can increase ECM synthesis by inhibiting the expression of GAS5 to relieve articular cartilage degeneration during OA.

In cartilages with OA, the homeostasis of cartilage ECM is disrupted and cells produce large quantities of MMPs (31). Type II collagen is one of the most important components of the ECM, accounting for ~90% of all types of collagen in the ECM and serves to provide tensile strength to the cartilage (32,33). MMPs accelerate the breakdown of collagen in the articular cartilage, which thins collagen fibers and promote cartilage

degeneration (34). MMP-9 and MMP-13 are important regulators of OA, since their expression was previously demonstrated to be elevated in patients with OA, which in turn reduced the expression of collagen and proteoglycans by activating other collagenases (35,36). According to the western blot analysis in the present study, the expression of MMP-9 and MMP-13 was found to be increased whereas the expression of type II collagen was decreased in IL-1β-treated chondrocytes, a trend that was reversed by lncRNA GAS5 knockdown. These results suggest that lncRNA GAS5 can promote the expression of MMP-9 and MMP-13 and be involved in cartilage degradation by cleaving type II collagen.

TIMPs are secretory proteins that function to inhibit MMPs and are present in the majority of organs and bodily fluids (37). The balance between ECM synthesis and degradation in the articular cartilage is typically disrupted in OA (38). One of the main reasons for this is the imbalance in the expression and activity of MMPs/TIMPs (39). Maintaining a healthy MMP/TIMP balance can prevent cartilage damage (40). In the present study, it was shown that IL-1β could increase the expression levels of MMPs whilst decreasing the expression of TIMPs in chondrocytes, resulting in the imbalance of the MMPs/TIMPs ratio to aggravate ECM degradation. Treatment of these chondrocytes with ABPS was able to reduce the expression of lncRNA GAS5, which in turn could decrease the ratio of MMPs/TIMPs. These results suggest that ABPS can promote ECM synthesis by modulating the balance between MMP and TIMP expression.

The present study showed that for the treatment of OA, ABPS could function at least in part by regulating the expression of lncRNA GAS5. Therefore, further studies will need to be performed to explore the regulatory mechanism of ABPS on lncRNA GAS5 in OA. GAS5 has a number of different variants produced by alternate splicing during transcription (41). In addition, serum starvation and rapamycin administration can increase the expression of lncRNA GAS5 through the mTOR pathway in T cells (42). However, the effects of ABPS on the transcription or alternate splicing of lncRNA GAS5 during OA remain unclear. Therefore, the mechanism of ABPS-induced downregulation of lncRNA GAS5 expression requires further exploration in future studies of OA.

To conclude, results from the present study suggest that lncRNA GAS5 can serve an important role in regulating chondrocyte cell physiology and in turn ECM homeostasis. In addition, it was shown that ABPS can preserve the articular cartilage structure in OA by downregulating the expression of lncRNA GAS5 and regulating the expression of ECM-associated proteins in chondrocytes. This suggests that ABPS can inhibit the expression of lncRNA GAS5 and maintain the homeostasis of ECM, ultimately delaying the process of cartilage degeneration in OA.

Acknowledgements

Not applicable.

Funding

The present study was supported by the National Natural Science Foundation of China (grant no. 82104888); Scientific Research Foundation for the High-level Talents Fujian University of Traditional Chinese Medicine (grant nos. X2019011-talents and X2021007-talents).

Availability of data and materials

The datasets used and/or analyzed during the current study are available from the corresponding author on reasonable request.

Authors' contributions

CLF, ZWQ and YFH performed the experiments and analyzed the data. YYM, QL, JWZ and WHZ performed the experiments. DZM designed the study and analyzed the data. CLF, ZWQ and YFH confirm the authenticity of all the raw data. All authors have read and approved the final version of the manuscript.

Ethics approval and consent to participate

All the experimental procedures were approved by the Animal Use and Care Committee of Fujian University of Chinese Traditional Medicine (approval no. 2019122; Fuzhou, China).

Patient consent for publication

Not applicable.

Competing interests

The authors declare that they have no competing interests.

References

1. Sharma L: Osteoarthritis of the Knee. N Engl J Med 384: 51-59, 2021.
2. Berenbaum F and Walker C: Osteoarthritis and inflammation: A serious disease with overlapping phenotypic patterns. Postgrad Med 132: 377-384, 2020.
3. Quicke JG, Conaghan PG, Corp N and Peat G: Osteoarthritis year in review 2021: Epidemiology & therapy. Osteoarthr Cartilage 30: 196-206, 2022.
4. Sun X, Zhang J, Li Y, Ren W and Wang L: Etomidate ameliorated advanced glycation end-products (AGEs)-induced reduction of extracellular matrix genes expression in chondrocytes. Bioengineered 12: 4191-4200, 2021.
5. Kumavat R, Kumar V, Malhotra R, Pandit H, Jones E, Ponchel F and Biswas S: Biomarkers of joint damage in osteoarthritis: Current status and future directions. Mediat Inflamm 2021: 5574582, 2021.
6. D Adamo S, Cetrullo S, Panichi V, Mariani E, Flamigni F and Borzì RM: Nutraceutical activity in osteoarthritis biology: A focus on the nutrigenomic role. Cells 9: 1232, 2020.
7. Stack J and McCarthy GM: Cartilage calcification and osteoarthritis: A pathological association? Osteoarthritis Cartilage 28: 1301-1302, 2020.
8. Xu XX, Zhang XH, Diao Y and Huang YX: Achyranthes bidentate saponins protect rat articular chondrocytes against interleukin-1β-induced inflammation and apoptosis in vitro. Kaohsiung J Med Sci 33: 62-68, 2017.
9. Yang J, Liu J, Jiao D, Zhang G, Qu C, Chen H, Chen C, Yu S and Xiangyanga L: Prediction of the molecular mechanism of eucommiae Cortex-Achyranthis bidentatae radix in the treatment of osteoarthritis: Network pharmacology and molecular docking. Drug Dev Ind Pharm 30: 1235-1247, 2021.
10. Fan S, Wang Y, Zhang Y, Wu Y and Chen X: Achyranthes bidentata Polysaccharide activates nuclear factor-Kappa B and promotes cytokine production in J774A.1 cells through TLR4/MyD88 signaling pathway. Front Pharmacol 12: 753599, 2021.

11. He X, Wang X, Fang J, Chang Y, Ning N, Guo H, Huang L and Huang X: The genus Achyranthes: A review on traditional uses, phytochemistry, and pharmacological activities. J Ethnopharmacol 203: 260-278, 2017.
12. Zhang D, Wang C, Hou X and Yan C: Structural characterization and osteoprotective effects of a polysaccharide purified from Achyranthes bidentata. Int J Biol Macromol 139: 1063-1073, 2019.
13. Li Z, Ma D, Peng L, Li Y, Liao Z and Yu T: Compatibility of Achyranthes bidentata components in reducing inflammatory response through Arachidonic acid pathway for treatment of osteoarthritis. Bioengineered 13: 1746-1757, 2022.
14. Yi J, Li X, Wang S, Wu T and Liu P: Steam explosion pretreatment of Achyranthis bidentatae radix: Modified polysaccharide and its antioxidant activities. Food Chem 375: 131746, 2022.
15. Yu F, Li X, Cai L, Li H, Chen J, Wong X, Xu H, Zheng C, Liu X and Ye H: Achyranthes bidentata polysaccharides induce chondrocyte proliferation via the promotion of the G1/S cell cycle transition. Mol Med Rep 7: 935-940, 2013.
16. Tu J, Huang W, Zhang W, Mei J and Zhu C: The emerging role of lncRNAs in chondrocytes from osteoarthritis patients. Biomed Pharmacother 131: 110642, 2020.
17. Gao ST, Yu YM, Wan LP, Liu ZM and Lin JX: LncRNA GAS5 induces chondrocyte apoptosis by down-regulating miR-137. Eur Rev Med Pharmacol Sci 24: 10984-10991, 2020.
18. Liu W, La AT, Evans A, Gao S, Yu Z, Bu D and Ma L: Supplementation with sodium butyrate improves growth and antioxidant function in dairy calves before weaning. J Anim Sci Biotechnol 12: 2, 2021.
19. Li X, Zhang Z, Liang W, Zeng J, Shao X, Xu L, Jia L, He X, Li H, Zheng C, *et al*: Tougu Xiaotong capsules may inhibit p38 MAPK pathway-mediated inflammation: In vivo and in vitro verification. J Ethnopharmacol 249: 112390, 2020.
20. Zhang M, Wang Y, Zhang Q, Wang C, Zhang D, Wan JB and Yan C: UPLC/Q-TOF-MS-based metabolomics study of the anti-osteoporosis effects of Achyranthes bidentata polysaccharides in ovariectomized rats. Int J Biol Macromol 112: 433-441, 2018.
21. Zhang S, Zhang Q, Zhang D, Wang C and Yan C: Anti-osteoporosis activity of a novel Achyranthes bidentata polysaccharide via stimulating bone formation. Carbohyd Polym 184: 288-298, 2018.
22. Unno H, Hasegawa M, Suzuki Y, Iino T, Imanaka-Yoshida K, Yoshida T and Sudo A: Tenascin-C promotes the repair of cartilage defects in mice. J Orthop Sci 25: 324-330, 2020.
23. Wakitani S, Goto T, Pineda SJ, Young RG, Mansour JM, Caplan AI and Goldberg VM: Mesenchymal cell-based repair of large, full-thickness defects of articular cartilage. J Bone Joint Surg Am 76: 579-592, 1994.
24. Wang P, Ye Y, Yuan W, Tan Y, Zhang S and Meng Q: Curcumin exerts a protective effect on murine knee chondrocytes treated with IL-1β through blocking the NF-κB/HIF-2α signaling pathway. Ann Transl Med 9: 940, 2021.
25. Hunter DJ and Bierma-Zeinstra S: Osteoarthritis. Lancet 393: 1745-1759, 2019.
26. Weng X, Lin P, Liu F, Chen J, Li H, Huang L, Zhen C, Xu H, Liu X, Ye H and Li X: Achyranthes bidentata polysaccharides activate the Wnt/β-catenin signaling pathway to promote chondrocyte proliferation. Int J Mol Med 34: 1045-1050, 2014.
27. Wang J, Sun Y, Liu J, Yang B, Wang T, Zhang Z, Jiang X, Guo Y and Zhang Y: Roles of long noncoding RNA in osteoarthritis (Review). Int J Mol Med 48: 133, 2021.
28. Jiang S, Liu Y, Xu B, Zhang Y and Yang M: Noncoding RNAs: New regulatory code in chondrocyte apoptosis and autophagy. Wires RNA 11: e1584, 2020.
29. Xing D, Liang JQ, Li Y, Lu J, Jia HB, Xu LY and Ma XL: Identification of long noncoding RNA associated with osteoarthritis in humans. Orthop Surg 6: 288-293, 2014.
30. Tan L, Xie Y, Yuan Y and Hu K: LncRNA GAS5 as miR-26a-5p sponge regulates the PTEN/PI3K/Akt axis and affects extracellular matrix synthesis in degenerative nucleus pulposus cells in vitro. Front Neurol 12, 2021.
31. Lucafò M, Pugnetti L, Bramuzzo M, Curci D, Di Silvestre A, Marcuzzi A, Bergamo A, Martelossi S, Villanacci V, Bozzola A, *et al*: Long non-coding RNA GAS5 and intestinal MMP2 and MMP9 expression: A translational study in pediatric patients with IBD. Int J Mol Sci 20: 5280, 2019.
32. Zhang X, Dong Y, Dong H, Cui Y, Du Q, Wang X, Li L and Zhang H: Telmisartan mitigates TNF-α-induced Type II collagen reduction by upregulating SOX-9. ACS Omega 6: 11756-11761, 2021.
33. Majumdar MK, Askew R, Schelling S, Stedman N, Blanchet T, Hopkins B, Morris EA and Glasson SS: Double-knockout of ADAMTS-4 and ADAMTS-5 in mice results in physiologically normal animals and prevents the progression of osteoarthritis. Arthritis Rheum 56: 3670-3674, 2007.
34. Cui N, Hu M and Khalil RA: Biochemical and biological attributes of matrix metalloproteinases. Prog Mol Biol Transl Sci 147: 1-73, 2017.
35. Ma X, Zhang Z, Shen M, Ma Y, Li R, Jin X, Gao L and Wang Z: Changes of type II collagenase biomarkers on IL-1β-induced rat articular chondrocytes. Exp Ther Med 21: 582, 2021.
36. Slovacek H, Khanna R, Poredos P, Poredos P, Jezovnik M, Hoppensteadt D, Fareed J and Hopkinson W: Interrelationship of MMP-9, Proteoglycan-4, and inflammation in osteoarthritis patients undergoing total hip arthroplasty. Clin Appl Thromb Hemost 27: 1076029621995569, 2021.
37. Jackson HW, Defamie V, Waterhouse P and Khokha R: TIMPs: Versatile extracellular regulators in cancer. Nat Rev Cancer 17: 38-53, 2017.
38. Rahmati M, Nalesso G, Mobasheri A and Mozafari M: Aging and osteoarthritis: Central role of the extracellular matrix. Ageing Res Rev 40: 20-30, 2017.
39. Sang W, Xue S, Jiang Y, Lu H, Zhu L, Wang C and Ma J: METTL3 involves the progression of osteoarthritis probably by affecting ECM degradation and regulating the inflammatory response. Life Sci 278: 119528, 2021.
40. Iannone F and Lapadula G: The pathophysiology of osteoarthritis. Aging Clin Exp Res 15: 364-372, 2003.
41. Zhou Z, Chen J, Huang Y, Liu D, Chen S and Qin S: Long noncoding RNA GAS5: A new factor involved in bone diseases. Front Cell Dev Biol 9: 807419, 2022.
42. Mourtada-Maarabouni M, Hasan AM, Farzaneh F and Williams GT: Inhibition of human T-Cell proliferation by mammalian target of rapamycin (mTOR) antagonists requires noncoding RNA growth-arrest-specific transcript 5 (GAS5). Mol Pharmacol 78: 19-28, 2010.

This work is licensed under a Creative Commons Attribution-NonCommercial-NoDerivatives 4.0 International (CC BY-NC-ND 4.0) License.